Simulating the Volcanic Sulfate Aerosols from the 1991 Eruption of Cerro Hudson and their Impact on the 1991 Ozone Hole

Parker A. Case[1,2], Peter R. Colarco[2], O. Brian Toon[3], Paul A. Newman[2]

[1]Oak Ridge Associated Universities, Oak Ridge, TN

[2]NASA GSFC, Greenbelt, MD, United States

[3]University of Colorado Boulder, Boulder, CO, United States

Corresponding author: Parker A. Case (parker.a.case@nasa.gov)

Key Points:

- The August 1991 eruption of Cerro Hudson is simulated using a model with detailed aerosol microphysics and stratospheric chemistry.
- The model shows skill in simulating the satellite and in-situ observations of the volcanic plume.
- These simulations present a prima facie case that this eruption contributed to the anomalously high 1991 Austral Springtime ozone loss.

Abstract

The Chilean volcano Cerro Hudson erupted between August 8th and 15th, 1991, injecting between 1.7 and 2.9 Tg of SO_2 into the upper troposphere and lower stratosphere. We simulate this injection using the GEOS Earth system model with detailed sulfur chemistry and sectional aerosol microphysics, focusing on the resulting aerosols and their contribution to the 1991 Antarctic Austral Springtime ozone hole. The simulations show a column ozone deficit (12 DU) in the Southern Hemisphere vortex collar region. The majority of this effect is between 10 and 20 km and due to heterogeneous chemistry. The model shows a 26% decrease in ozone from background levels at these altitudes, compared with in-situ observations of a 50% decrease. Above 20 km, the dynamical response to the eruption also causes lower ozone values, a novel modeling result. This experiment highlights potential interactions between proposed solar radiation management geoengineering aerosols and volcanic eruptions.

Plain Language Summary

We simulated the August, 1991 eruption of Chilean volcano Cerro Hudson. Cerro Hudson erupted two months after the June 15th eruption of Pinatubo which was one of the largest observed eruptions. The combination of these two eruptions impacted the atmosphere by injecting volcanic aerosol which are well represented by our model. In the case of Cerro Hudson, the simulations show that the volcanic plume may have impacted the 1991 Antarctic ozone hole, both by directly impacting the chemistry of ozone depletion and by altering the dynamics of the atmosphere, slowing down the normal breakdown of the ozone hole caused by changes in weather. The interaction between Cerro Hudson and Pinatubo shown here also reveal a need for more research in how potential goengineering scenarios would interact with volcanic eruptions.

1 Introduction

While the August 8th to 15th Cerro Hudson (45°S, 72°W) volcanic eruption produced the fifth largest sulfur dioxide (SO_2) emissions ever observed by satellites, it was overshadowed by the June 15th Mount Pinatubo (15°N, 120°E) eruption (Carn et al., 2016). The Cerro Hudson injection is estimated to have put 1.7-2.9 Tg of SO_2 and a similar amount of ash between 16-18 km (Bluth et al., 1992; Constantine et al., 2000; Miles et al., 2017). The ash and SO_2 quickly separated, with about 90% of the ash falling out in the first few days following the eruption, settling across South America (Constantine et al., 2000). The SO_2 was observed by the Total Ozone Mapping Spectrometer (TOMS) (Bluth et al., 1992) and High Resolution Infra-Red Radiation Sounder/2 (HIRS/2) (Miles et al., 2017) satellite instruments and remained in the lower stratosphere between 50°S and 70°S as it circled the Earth (Fig. 1b and c; Doiron et al., 1991; Schoeberl et al., 1993). The satellite-borne Microwave Limb Sounder (MLS), also capable of retrieving SO_2, came online in September 1991, and while it was able to make useful observations of the tropical Pinatubo plume, produced noisy results at the altitude and latitude of the Cerro Hudson plume (Miles et al., 2017).

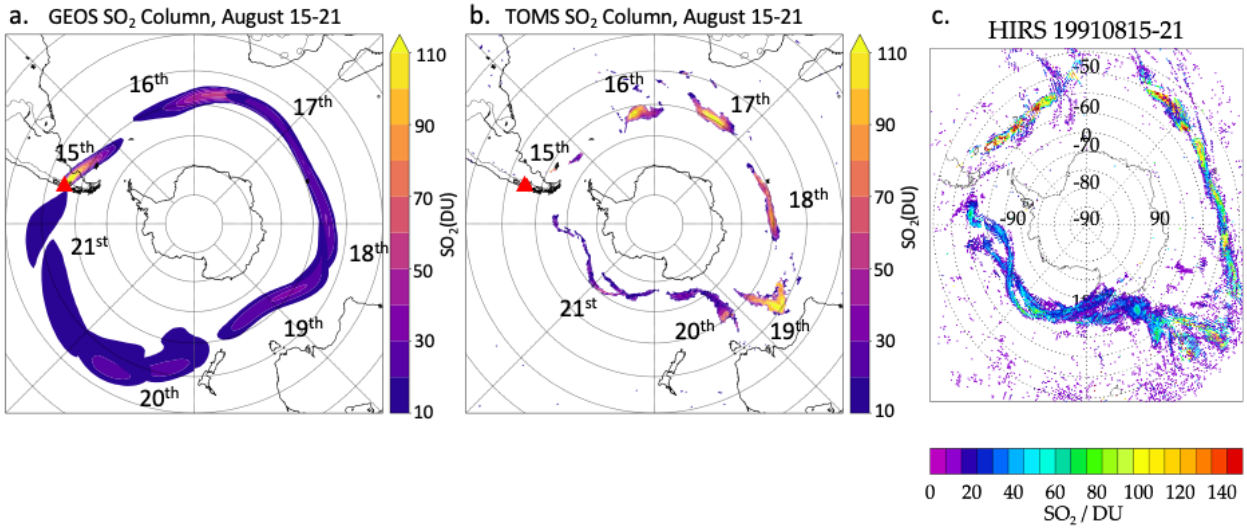

Figure 1: Seven-day composite of one instance of model calculated (a) and satellite retrieved (TOMS, b, and HIRS/2, c) SO_2 column concentrations as the Cerro Hudson plume transits the Southern midlatitudes. The observations from August 15th-21st are shown moving clockwise around Antarctica. (c) is from Miles et al., 2017.

On September 10th and daily after September 20th, the Cerro Hudson plume was observed above McMurdo Bay by both lidar and balloon-borne optical particle counter (Deshler et al., 1992; Hofmann et al., 1993). The low altitude of the volcanic aerosol layer, between 9 and 13 km, combined with the presence of freshly nucleated aerosols, indicated that this aerosol was from Cerro Hudson. The Pinatubo plume, on the other hand, was detected only above 17 km. Deshler et al. (1992) and Hofmann et al. (1993) found coincident low ozone measurements at 12 km, where ozone concentrations are normally not impacted by seasonal depletion. They reported an ozone loss rate of 4-8 ppb day^{-1} over 30 days following September 24th, totaling ~50% ozone depletion compared to years with comparable PSC-induced ozone loss. Despite these in-situ observations of aerosols and anomalous ozone values, satellite observations did not show the Cerro Hudson SO_2 entering the vortex before the beginning of September (Krueger et al., 1992). Trajectory model results also suggested that the volcanic plume remained outside of the vortex during the period of major ozone depletion (Krueger et al., 1992, Schoeberl et al., 1993).

Studies of more recent volcanic eruptions occurring in the Southern midlatitudes show that even moderately sized eruptions at these latitudes can impact the springtime ozone loss (Solomon et al., 2016; Zhu et al., 2018). In the case of the April 2015 Calbuco eruptions (Zhu et al., 2018), observations and models show that transport of volcanic aerosols into the vortex occurred as early as May, allowing them to alter polar stratospheric clouds and the chemistry of springtime ozone depletion. Despite a later eruption date, Deshler et al. (1992) showed that Cerro Hudson aerosol appeared at high Southern latitudes and potentially impacted ozone in September and October.

We simulated the 1991 Cerro Hudson eruption using the Goddard Earth Observing System (GEOS) model coupled with a sectional aerosol microphysics module, the Community Aerosol and Radiation Model for Atmospheres (CARMA), and the tropospheric and stratospheric chemistry module GEOS-Chem (GC). Here we show that (i) the GEOS model

reasonably reproduces the satellite and balloon-borne in-situ observations of the Cerro Hudson plume, (ii) Cerro Hudson aerosol reached high Southern latitudes and impacted ozone below 20 km while remaining outside the vortex above 20 km, and (iii) the dynamical response to these aerosols resulted in a more persistent vortex and lower ozone values above 20 km.

2 Materials and Methods

GEOS is an Earth system model based on the architecture of the Earth System Modeling Framework (ESMF) (Hill et al., 2004; Molod et al., 2015). In this study, we use the atmospheric general circulation model (AGCM) configuration in its "free-running" mode, in which the model calculates its own meteorology without any data assimilation and with imposed sea surface temperatures based on observations. The GEOS system has been shown to perform well in stratospheric chemistry and transport processes (SPARC CCMVal, 2010; Strahan et al., 2011; Douglass et al., 2012). We run GEOS at a ~100 km horizontal resolution on a cubed-sphere grid with 72 hybrid-sigma vertical levels extending from the surface to ~80 km. While the GEOS AGCM can be coupled to various aerosol modules, here we are using the sectional aerosol microphysics from CARMA (Toon et al., 1988; Bardeen et al., 2008; Colarco et al. 2014). We have coupled CARMA to the GEOS-Chem tropospheric and stratospheric chemistry mechanism (Bey et al., 2001)—GEOS-Chem calculates the production of H_2SO_4 gas, which CARMA then uses to calculate the aerosol microphysics across a range of size bins. Both CARMA and GEOS-Chem are radiatively interactive within the model. For a complete description of GEOS-Chem, CARMA, radiative calculations, and the coupling of the GEOS model, see Case et al. (2023).

Three 3-member ensembles are used in this study. The first 3-member ensemble is a background ensemble representing the second half of 1991 without the Pinatubo or Cerro Hudson eruptions. The second ensemble includes only the Pinatubo eruption over the same period, and the final ensemble includes both the Pinatubo and Cerro Hudson eruptions. Ensemble members are perturbed at the beginning of 1991 to develop varying meteorological and dynamical situations.

Cerro Hudson is initialized in the model with an injection of 2.7 Tg of SO_2 between 16 and 18 km in the grid column above the volcano, spread out over 24 hours on the day of the largest eruption (August 15). We use Pinatubo injection parameters similar to those in Mills et al. (2017): we inject 10 Tg SO_2 over 25 hours on June 15, 1991, uniformly mixed from 18 to 21 km altitude between 0° and 15°N over a 1-degree wide longitude region centered at 120°E. This configuration is identical to the simulations presented and validated in Case et al. (2023).

3 Results and Discussion

The GEOS model (Fig. 1a) shows similar transport and SO_2 magnitude to that observed by TOMS (Fig. 1b) and HIRS/2 (Fig. 1c) for the six days after the Cerro Hudson eruption. An average peak value of 109 DU in the model is slightly lower than the 130+ DU peak in observations. By the time the plume returned to the longitude of the volcano, the modeled plume has a peak SO_2 column of 16 DU while columns as high as 50 DU were observed by both instruments. The horizontal extent of the plume is wider in the model, indicating the lower peak values are in part due to the spatial resolution of the model compared to the observations.

The model-calculated late-September zonal mean aerosol size distribution at 11 km at the latitude of McMurdo Bay, Antarctica (78°S), shows an enhancement by a factor of 3 in the total particle number concentration in the ensemble that includes Cerro Hudson. Particle size also

increases when Cerro Hudson is included, from an effective radius of 0.12 μm to 0.16 μm, representative of young volcanic plumes. This magnitude of enhancement in the number concentration and size of aerosols is consistent with the anomalous aerosol layer observed at 11 km by Deshler et al. (1992) above McMurdo Bay on September 27th relative to earlier balloon flights (Fig. 2).

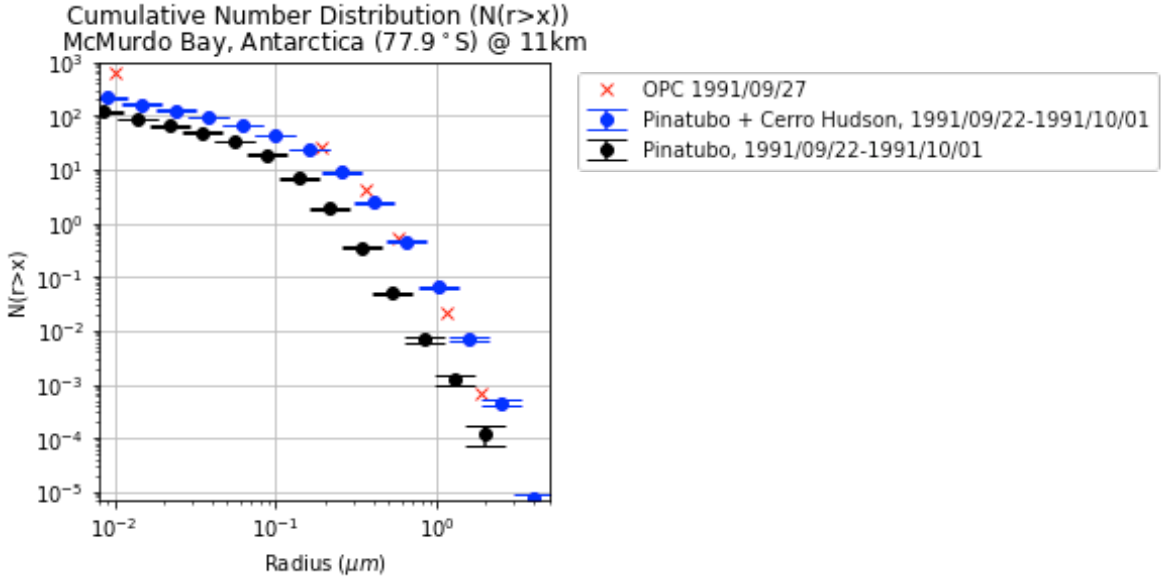

Figure 2: Balloon-borne optical particle counter observations above McMurdo Bay on September 27th (red Xs), compared with model-calculated late-September zonal-mean cumulative aerosol size distributions at the latitude of McMurdo for the ensemble including Cerro Hudson (blue dots with error bars) and the ensemble excluding Cerro Hudson (black dots with error bars). Error bars represent the 95% confidence interval across each ensemble.

Starting in late September, the ensemble including Cerro Hudson has a 5-10% larger ozone hole area, defined as the area inside the 220 DU contour, continuing throughout October (Fig. 3). It should be noted that the model-calculated ozone hole area is larger than observed 1991 values due to a model low bias of polar ozone. The recovery of ozone values in the ensemble including Cerro Hudson is slowed by an average of 13 days throughout October. The extra ozone hole area in the simulations with Cerro Hudson is primarily driven by lower ozone values in the "collar region", defined here as the longitudinal ring around the Ozone Hole between 55°S and 65°S. The model shows 20-40% lower ozone in the collar region between 10 km to 25 km when Cerro Hudson is included (Fig. 4c).

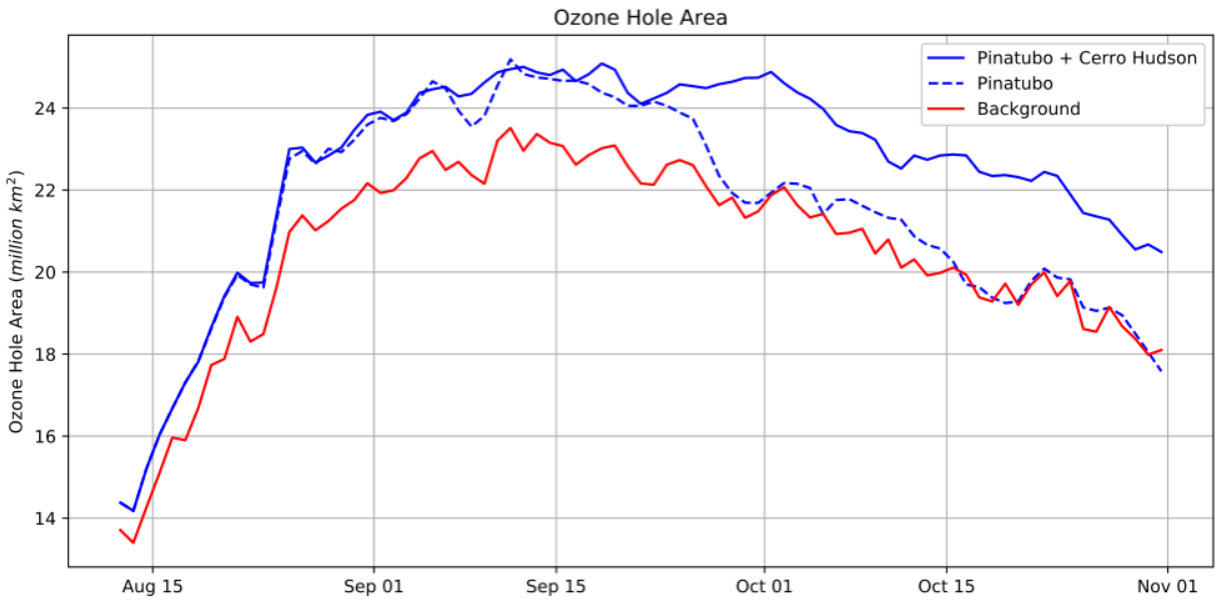

Figure 3: Ozone hole area (defined as the area contained by the 220 DU total ozone value) in the GEOS model for the ensemble including Cerro Hudson (solid blue), ensemble excluding Cerro Hudson (dashed blue), and the background excluding both eruptions (solid red).

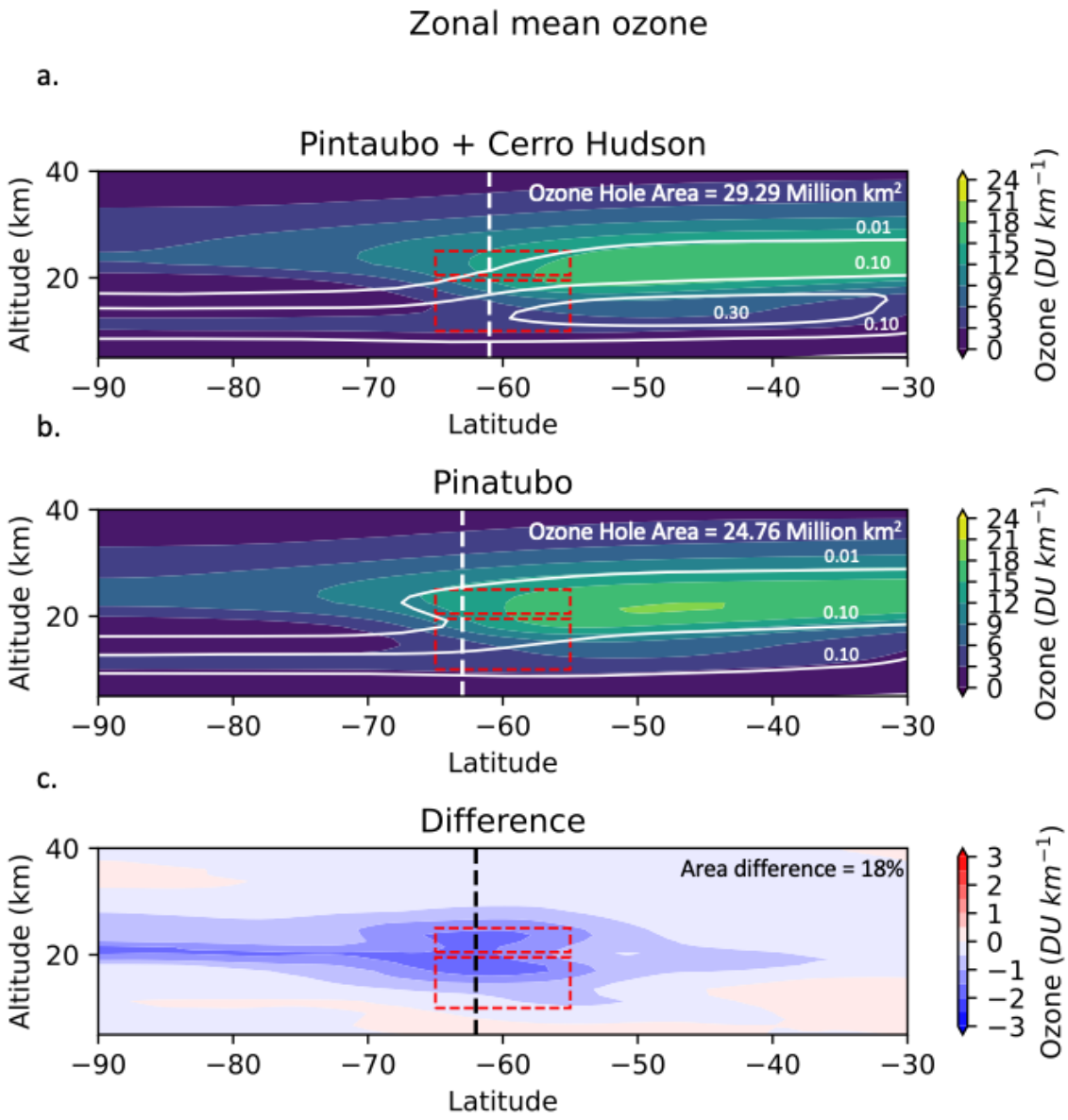

Figure 4: Zonal mean ozone concentrations and sulfate aerosol surface area densities (cm^2 m^{-3}) in the GEOS modeled Southern Hemisphere (DU/km). In filled contours are the ozone fields and in white contours are the aerosol surface area fields for the ensemble including Cerro Hudson (a), the ensemble excluding Cerro Hudson (b), and the difference (c). The dotted white line on each figure indicates the vortex edge. The dotted red lines indicate the upper and lower collar regions.

The development of this low-ozone collar region in the ensemble including Cerro Hudson is coincident with the start of lower temperatures when compared with the ensemble without Cerro Hudson (Fig. 5). The ensembles meaningfully diverge starting in late September. While there is a small amount of volcanic aerosol surface area from Pinatubo in the region prior to this divergence, once the ensembles diverge, there is less aerosol surface area between 20 and 25 km in the ensemble including Cerro Hudson (Figs. 5a, 4), despite a higher volcanic aerosol loading between 10 and 20 km in that ensemble (Figs. 5b, 4).

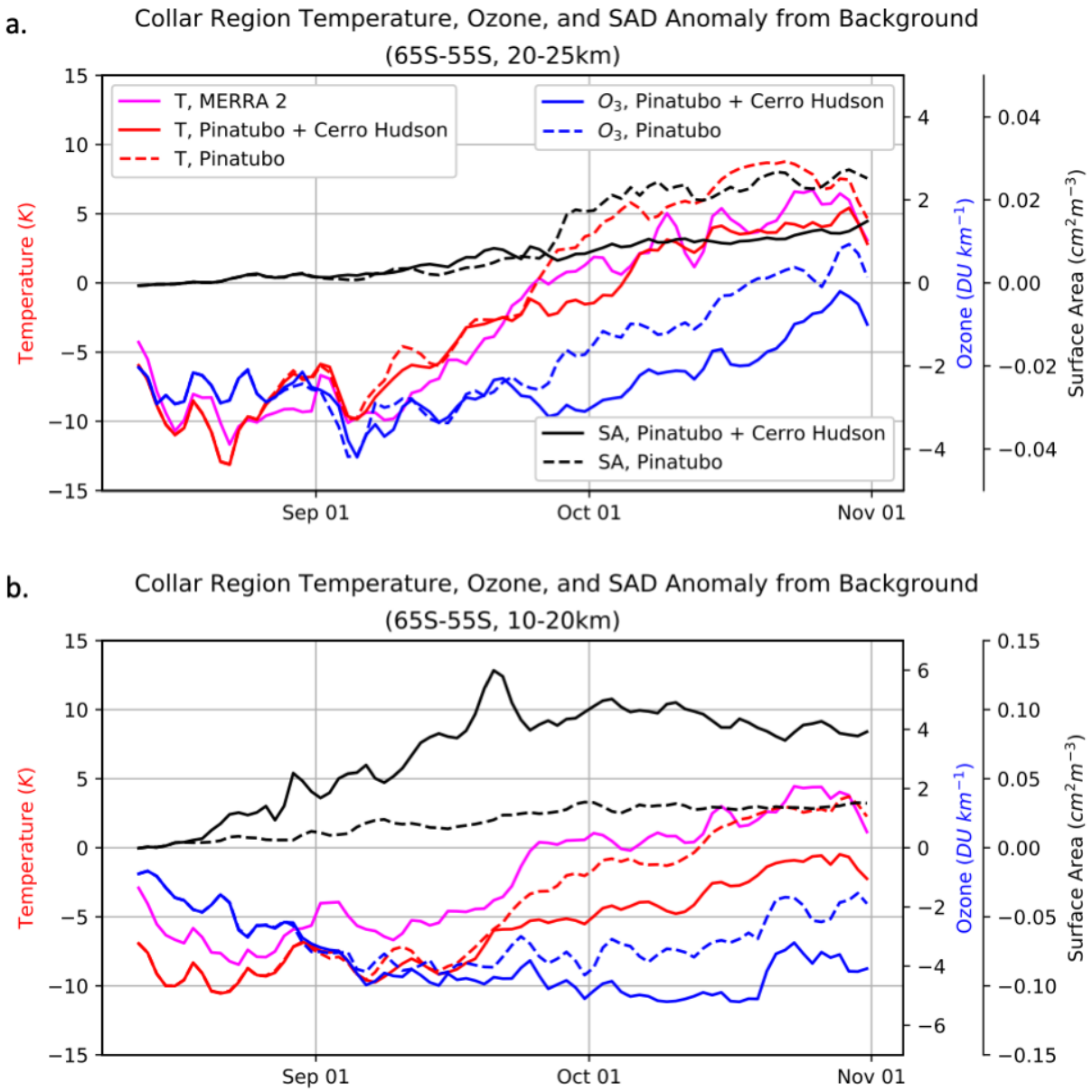

Figure 5: Modeled temperature (red), ozone (blue), and surface area (black) anomalies with respect to the background versus time in the polar vortex collar region (55°S to 65°S) for: (a) 20-25 km, and (b) 10-20 km. Zero values indicate that ensembles are similar to the background ensemble, while negative anomalies indicate colder temperatures, lower ozone concentrations, and lower surface area. MERRA-2 temperatures are shown in pink.

The differences in ozone concentrations above 20 km were not driven by a change in the heterogeneous component of the ozone chemistry, evidenced by the lack of volcanic aerosol at that altitude (Fig. 5a). Ozone depletion at these altitudes mainly occurs during August and September where only small aerosol enhancements are noted. The lower temperatures compared to the background at 20-25 km in both ensembles point instead to a dynamical perturbation as the causal factor for lower ozone values. By comparison, below 20 km (Fig. 5b), the additional

aerosol surface area in the ensemble including Cerro Hudson is coincident with the lower ozone values, indicating extra heterogeneous activation of ozone depleting substances.

Ozone near the edge of the vortex is driven primarily by tropospheric wave forcing of the stratosphere (Newman et al., 2004). Eddy heat flux (Fig. 6a), the product of temperature and the meridional wind component anomalies from the zonal mean, is proportional to planetary wave energy that propagates vertically into the stratosphere (Edmon et al., 1980) and has been shown to drive temperature and ozone concentrations near the edge of the vortex by controlling vertical motions in the polar lower stratosphere (Newman et al., 2001; Newman et al., 2004). Negative values from September 13-19 (3-5 days before the ensembles diverge in ozone in the collar region) indicate a wave event in the ensemble without Cerro Hudson across the three members. In the Southern Hemisphere, a negative eddy heat flux means increased downward motion in the vortex collar, increasing temperatures and ozone in the polar lower stratosphere. This suggests that the radiative impact of the Cerro Hudson aerosol layer acts to reduce tropospheric wave activity propagating into the stratosphere, resulting in a colder lower ozone collar region above the layer of Cerro Hudson aerosols. Radiative heating of the Cerro Hudson aerosols in the midlatitudes also increases the temperature gradient at the altitude of the Antarctic vortex, associated with a stronger zonal wind (Fig. 6b). This results in the longer-lasting isolated vortex in the ensemble including Cerro Hudson.

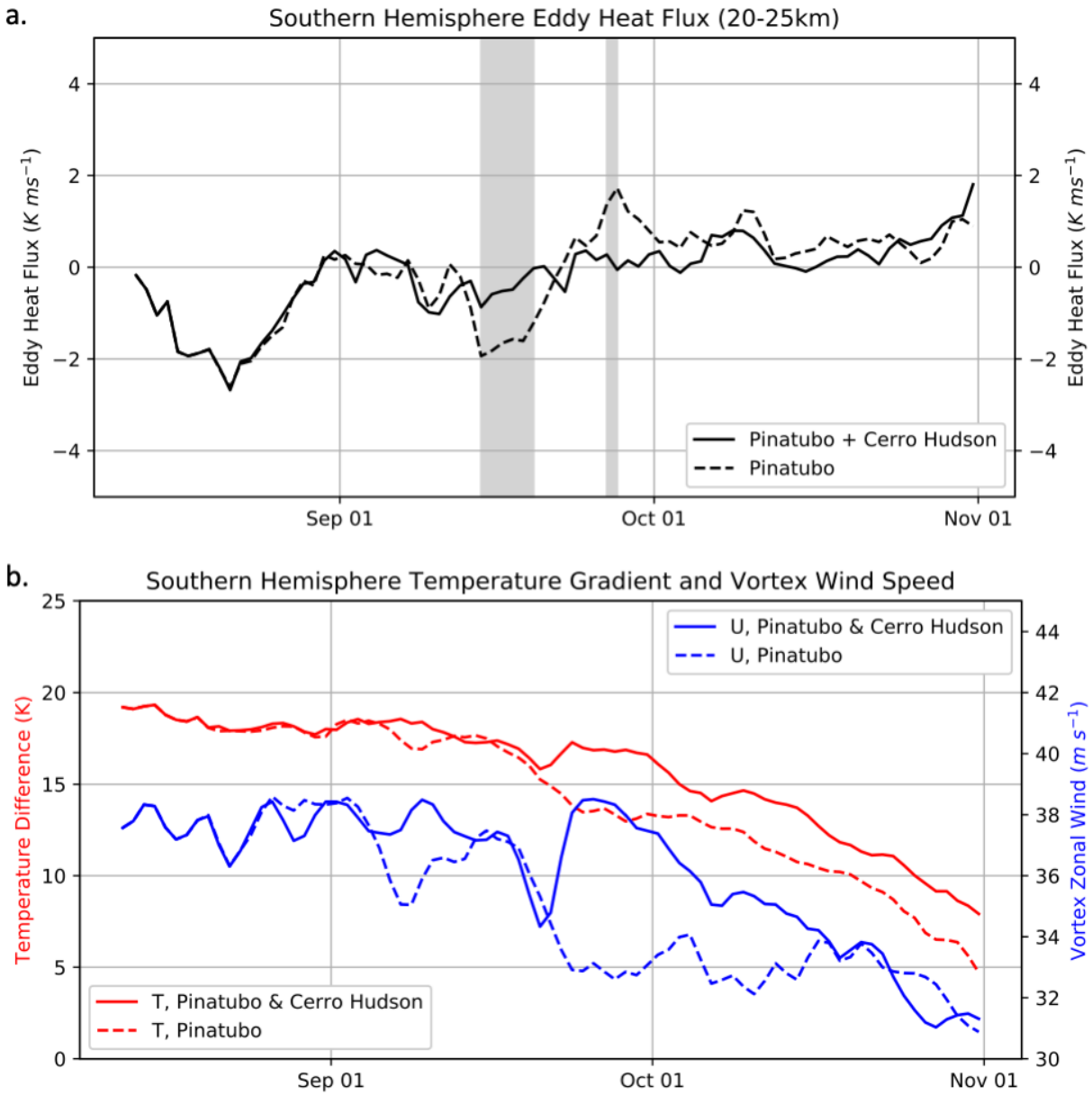

Figure 6: (a) Southern hemisphere eddy heat flux for the ensemble mean with Cerro Hudson (solid line) and the ensemble mean without Cerro Hudson (dashed line). The shaded area indicates days when the ensemble memberss do not overlap. (b) (Red) Southern hemisphere poleward temperature gradient, calculated as the temperature difference between the region between 15°S and 30°S and the region between 60°S and 90°S, between 10 and 30 km. (Blue) Southern hemisphere vortex zonal wind speed, defined as the wind spead averaged from 10-20 km, 40°-60° S.

4 Conclusions

The free-running GEOS model shows that the direct radiative impact of the August 15, 1991, Cerro Hudson eruption may have altered the dynamics of the Southern Hemisphere, suppressing tropospheric wave propagation into the stratosphere. This suppression cools the

Antarctic lower stratosphere, increases the temperature difference between low latitudes and the pole, and strengthens the vortex. The suppression also results in a slower breakdown of the Antarctic vortex than would have otherwise occurred. Ultimately, this dynamical forcing of the lower stratosphere in the model results in lower ozone within the collar region in late September and October above 20 km. While this dynamical impact is consistent across all ensemble members in this study, a larger ensemble size is needed to strengthen these findings.

GEOS includes coupling between the volcanic aerosols and chlorine and bromine activation, but the model simulations show little volcanic aerosol present above 20 km during the peak ozone hole depletion period. Based on these results, the aerosols from Pinatubo and Cerro Hudson did not directly change ozone chemistry in the 1991 Antarctic vortex above 20 km. The modeled Cerro Hudson aerosols did penetrate the Antarctic stratospheric region in a layer near 15 km (below the primary PSC-driven ozone depletion region). At this altitude, surface area in the model is increased by more than an order of magnitude, where it causes some additional ozone depletion.

The combined dynamical and chemical impacts cause 12 DU less column ozone in the collar region with respect to the GEOS background ensemble—increasing the ozone hole area by an average of 9% in October. Between 20 km and 25 km, local ozone is decreased by an average of 1.3 DU/km (0.37 ppmv, 11%) in October from background levels. The region between 10 km and 20 km in the model shows a decrease of 1.5 DU/km (0.11 ppmv, 26%). Ozone in this region was observed to decrease by 50% by Deshler et al., 1992, consistent with both the satellite observations of ozone from late September through October 1991 (Kreuger et al., 1992) and the in-situ aerosol and ozone measurements of Hofmann et al., 1993. We have focused here on the impact on the 1991 ozone hole, but the increasing aerosol surface area in the collar region in Fig. 5 show that the Pinatubo aerosols may have impacted the ozone hole in subsequent years, as has been shown by modeling and observational studies (Hofmann et al., 1993; Knight et al., 1998; Stenchikov et al., 2002).

Finally, the Cerro Hudson impact is deeply convolved with the Pinatubo impact. The GEOS simulations show an anomalously cold and persistent vortex prior to the impact of Cerro Hudson in late September. In the collar region specifically, ozone concentrations were 2.5 DU/km (0.71 ppmv) lower than the background and had recovered to background values from the Pinatubo-caused anomaly above 20 km by October 16th. A similar lag is seen between 10 km and 20 km. Temperature in the collar region in August is 7.8 K colder in both ensembles when compared to background values indicating Pinatubo's role in the stability of the Antarctic vortex. These results could also have relevance to potential geoengineering scenarios, highlighting the potential interactions between solar radiation management aerosols and volcanic eruptions. The divergent chemical and radiative impacts of Pinatubo and Cerro Hudson shown here need to be studied in the context of volcanic eruptions occurring during an ongoing geoengineering scheme.

Acknowledgments

This work was carried out under funding from the NASA Modeling, Analysis, and Prediction (MAP) program (PM: David Considine) under the Chemistry-Climate Modeling project, a NASA FINESST proposal (PI: Brian Toon) entitled "Using GEOS-5/CARMA to improve interpretations of NASA satellite observations of stratospheric aerosols", and a NASA Postdoctoral Fellowship (PI: Pete Colarco) "Towards a more complete representation of

stratospheric aerosols in the GEOS Earth System Model". Simulations were carried out using high-performance computing resources provided by the NASA Center for Climate Simulation (NCCS).

Open Research

Original model output for this study has been published (Case, 2023). Other data used in the analysis includes: MERRA 2 (Gelaro et al., 2017); TOMS SO2 data (Krotkov et al., 2019); HIIRS/2 data from Miles et al., 2017; and University of Wyoming OPC data (Deshler et al., 2019).

References

Aquila, V., Oman, L.D., Stolarski, R.S., Colarco, P.R. and Newman, P.A., 2012. Dispersion of the volcanic sulfate cloud from a Mount Pinatubo–like eruption. *Journal of Geophysical Research: Atmospheres*, *117*(D6).

Bardeen, C.G, O.B. Toon, E.J. Jensen, D.R. Marsh, and V.L. Harvey, 2008. Numerical simulations of the three-dimensional distribution of meteoric dust in the mesosphere and upper stratosphere. *Journal of Geophysical Research: Atmospheres, 113, D17202, doi:10.1029/2007JD009515.*

Bey, I., Jacob, D.J., Yantosca, R.M., Logan, J.A., Field, B.D., Fiore, A.M., Li, Q., Liu, H.Y., Mickley, L.J. and Schultz, M.G., 2001. Global modeling of tropospheric chemistry with assimilated meteorology: Model description and evaluation. *Journal of Geophysical Research: Atmospheres*, *106*(D19), pp.23073-23095.

Bluth, G.J., Doiron, S.D., Schnetzler, C.C., Krueger, A.J. and Walter, L.S., 1992. Global tracking of the SO_2 clouds from the June, 1991 Mount Pinatubo eruptions. *Geophysical Research Letters*, *19*(2), pp.151-154.

Carn, S.A., Clarisse, L. and Prata, A.J., 2016. Multi-decadal satellite measurements of global volcanic degassing. *Journal of Volcanology and Geothermal Research*, *311*, pp.99-134.

Case, Parker. (2023). Data for Simulating the Volcanic Sulfate Aerosols from the 1991 Eruption of Cerro Hudson and their Impact on the 1991 Ozone Hole (1.0) [Dataset]. Zenodo. *doi:10.5281/zenodo.8384145*

Case, P.C., Colarco, P.R., Toon, O.B., Aquila, V., and Keller, C.A., 2023. Interactive stratospheric aerosol microphysics-chemistry simulations of the 1991 Pinatubo volcanic aerosols with newly coupled sectional aerosol and stratosphere-troposphere chemistry modules in the NASA GEOS Chemistry-Climate Model (CCM). *Journal of Advancements in Modeling Earth Systems* 15, no. 8 (2023): e2022MS003147.

Colarco, P.R., Nowottnick, E.P., Randles, C.A., Yi, B., Yang, P., Kim, K.M., Smith, J.A. and Bardeen, C.G., 2014. Impact of radiatively interactive dust aerosols in the NASA GEOS-5 climate model: Sensitivity to dust particle shape and refractive index. *Journal of Geophysical Research: Atmospheres*, *119*(2), pp.753-786.

Constantine, E. K., Bluth, G. J., & Rose, W. I. (2000). TOMS and AVHRR observations of drifting volcanic clouds from the August 1991 eruptions of Cerro Hudson. *Washington DC American Geophysical Union Geophysical Monograph Series*, *116*, 45-64.

Deshler, T., Adriani, A., Gobbi, G.P., Hofmann, D.J., Di Donfrancesco, G. and Johnson, B.J., 1992. Volcanic aerosol and ozone depletion within the Antarctic polar vortex during the austral spring of 1991. *Geophysical research letters*, *19*(18), pp.1819-1822.

Deshler, T., Luo, B., Kovilakam, M., Peter, T. and Kalnajs, L.E., 2019. Retrieval of aerosol size distributions from in situ particle counter measurements: Instrument counting efficiency and comparisons with satellite measurements. *Journal of Geophysical Research: Atmospheres*, *124*(9), pp.5058-5087. *doi:10.1029/2018JD029558*

296 Doiron, S. D., Bluth, G. J., Schnetzler, C. C., Krueger, A. J., & Walter, L. S. (1991). Transport of
297 Cerro Hudson SO2 clouds. *Eos, Transactions American Geophysical Union*, *72*(45), 489-498.
298 Douglass, A. R., R. S. Stolarski, S. E. Strahan, and L. D. Oman, 2012. Understanding differences
299 in upper stratospheric ozone response to changes in chlorine and temperature as computed using
300 CCMVal-2 models. *Journal of Geophysical Research: Atmospheres*, *117, D16306,*
301 *doi:10.1029/2012JD017483.*
302 English, J.M., Toon, O.B. and Mills, M.J., 2013. Microphysical simulations of large volcanic
303 eruptions: Pinatubo and Toba. *Journal of Geophysical Research: Atmospheres*, *118*(4), pp.1880-
304 1895.
305 Gelaro, R., McCarty, W., Suárez, M.J., Todling, R., Molod, A., Takacs, L., Randles, C.A.,
306 Darmenov, A., Bosilovich, M.G., Reichle, R. and Wargan, K., 2017. The modern-era
307 retrospective analysis for research and applications, version 2 (MERRA-2). *Journal of climate*,
308 *30*(14), pp.5419-5454.
309 Hill, C., DeLuca, C., Suarez, M. and Da Silva, A., 2004. The architecture of the earth system
310 modeling framework. *Computing in Science & Engineering*, *6*(1), pp.18-28.
311 Hofmann, D.J. and Oltmans, S.J., 1993. Anomalous Antarctic ozone during 1992: Evidence for
312 Pinatubo volcanic aerosol effects. *Journal of Geophysical Research: Atmospheres*, *98*(D10),
313 pp.18555-18561.
314 Knight, J.R., Austin, J., Grainger, R.G. and Lambert, A., 1998. A three-dimensional model
315 simulation of the impact of Mt. Pinatubo aerosol on the Antarctic ozone hole. *Quarterly Journal*
316 *of the Royal Meteorological Society*, *124*(549), pp.1527-1558.

317 Kovilakam, M., Thomason, L.W., Ernest, N., Rieger, L., Bourassa, A. and Millán, L., 2020. The
318 global space-based stratospheric aerosol climatology (version 2.0): 1979–2018. *Earth System*
319 *Science Data*, *12*(4), pp.2607-2634.
320 Krotkov N.A., Bhartia, P.K., Fisher, B., Leonard, P., 2019. TOMS/N7 MS SO2 Vertical Column
321 1-Orbit L2 Swath 50x50 km V3 [Dataset]. Goddard Earth Sciences Data and Information
322 Services Center (GES DISC). *doi:10.5067/MEASURES/SO2/DATA204*
323 Krueger, A., Schoeberl, M., Newman, P., & Stolarski, R. (1992). The 1991 Antarctic ozone hole;
324 TOMS observations. *Geophysical research letters*, *19*(12), 1215-1218.
325 Miles, G. M., Siddans, R., Grainger, R. G., Prata, A. J., Fisher, B., & Krotkov, N. (2017).
326 Retrieval of volcanic SO_2 from HIRS/2 using optimal estimation. *Atmospheric Measurement*
327 *Techniques*, *10*(7), 2687-2702.
328 Mills, M.J., Richter, J.H., Tilmes, S., Kravitz, B., MacMartin, D.G., Glanville, A.A., Tribbia,
329 J.J., Lamarque, J.F., Vitt, F., Schmidt, A. and Gettelman, A., 2017. Radiative and chemical
330 response to interactive stratospheric sulfate aerosols in fully coupled CESM1 (WACCM).
331 *Journal of Geophysical Research: Atmospheres*, *122*(23), pp.13-061.
332 Molod, A., Takacs, L., Suarez, M. and Bacmeister, J., 2015. Development of the GEOS-5
333 atmospheric general circulation model: Evolution from MERRA to MERRA2. *Geoscientific*
334 *Model Development*, *8*(5), pp.1339-1356.
335 Schoeberl, M. R., Doiron, S. D., Lait, L. R., Newman, P. A., & Krueger, A. J. (1993). A
336 simulation of the Cerro Hudson SO2 cloud. *Journal of Geophysical Research: Atmospheres*,
337 *98*(D2), 2949-2955.
338 Solomon, S., Ivy, D.J., Kinnison, D., Mills, M.J., Neely III, R.R. and Schmidt, A., 2016.
339 Emergence of healing in the Antarctic ozone layer. *Science*, *353*(6296), pp.269-274.

SPARC CCMVal. "SPARC Report on the Evaluation of Chemistry-Climate Models, edited by V." *Eyring, TG Shepherd, and DW Waugh, SPARC Rep* 5 (2010): 426.

Stenchikov, G., Robock, A., Ramaswamy, V., Schwarzkopf, M.D., Hamilton, K. and Ramachandran, S., 2002. Arctic Oscillation response to the 1991 Mount Pinatubo eruption: Effects of volcanic aerosols and ozone depletion. *Journal of Geophysical Research: Atmospheres*, *107*(D24), pp.ACL-28.

Strahan, Susan E., A. R. Douglass, R. S. Stolarski, H. Akiyoshi, Slimane Bekki, P. Braesicke, N. Butchart et al. "Using transport diagnostics to understand chemistry climate model ozone simulations." *Journal of Geophysical Research: Atmospheres* 116, no. D17 (2011).

Toon, O.B., Turco, R.P., Westphal, D., Malone, R. and Liu, M., 1988. A multidimensional model for aerosols: Description of computational analogs. *Journal of Atmospheric Sciences*, *45*(15), pp.2123-2144.

Zhu, Y., Toon, O.B., Kinnison, D., Harvey, V.L., Mills, M.J., Bardeen, C.G., Pitts, M., Bègue, N., Renard, J.B., Berthet, G. and Jégou, F., 2018. Stratospheric aerosols, polar stratospheric clouds, and polar ozone depletion after the Mount Calbuco eruption in 2015. *Journal of Geophysical Research: Atmospheres*, *123*(21), pp.12-308.